

Fincher-Burke spin excitations and ω/T scaling in insulating $\text{La}_{1.95}\text{Sr}_{0.05}\text{CuO}_4$

Wei Bao,¹ Y. Chen,^{2,3} K. Yamada,⁴ A. T. Savici,⁵ P. L. Russo,⁶ J. E. Lorenzo,⁷ and J.-H. Chung^{2,3}

¹Condensed Matter and Thermal Physics, Los Alamos National Laboratory, Los Alamos, NM 87545

²NIST Center for Neutron Research, National Institute of Standards and Technology, Gaithersburg, MD 20899

³Dept. of Materials Science and Engineering, University of Maryland, College Park, MD 20742

⁴Institute of Materials Research, Tohoku University, Sendai 980-8577, Japan

⁵Brookhaven National Laboratory, Upton, NY 11973

⁶TRIUMF, Vancouver, BC V6T 2A3, Canada

⁷Institut Néel, CNRS, BP 166X, F-38043, Grenoble, France

(Dated: November 27, 2018)

Insulating $\text{La}_{1.95}\text{Sr}_{0.05}\text{CuO}_4$ shares with superconducting cuprates the same Fincher-Burke spin excitations, which usually are observed in itinerant antiferromagnets. The local spectral function satisfies ω/T scaling above ~ 16 K for this incommensurate insulating cuprate. Together with previous results in commensurate insulating and incommensurate superconducting cuprates, these results further support the general scaling prediction for square-lattice quantum spin $S = 1/2$ systems. The width of incommensurate peaks in $\text{La}_{1.95}\text{Sr}_{0.05}\text{CuO}_4$ scales to a similar finite value as at optimal doping, strongly suggesting that they are similarly distant from a quantum critical point. They might both be limited to a finite correlation length by partial spin-glass freezing.

It is well known that the (π, π) peak of the Néel antiferromagnetic order of the parent compounds is replaced by a quartet of incommensurate peaks when cuprates are sufficiently doped to have become superconducting¹. The very recent excitement is that spin excitations measured in superconducting $\text{La}_{2-x}\text{Sr}_x\text{CuO}_4$ (LSCO) ($x = 0.10$ and 0.16)², $\text{YBa}_2\text{Cu}_3\text{O}_{6.6}$ (YBCO)³, as well as in the “stripe-ordered” $\text{La}_{1.875}\text{Ba}_{0.125}\text{CuO}_4$ with a suppressed T_C ⁴ share a common spectral feature: broad excitation continua, originating from the incommensurate quartet, disperse towards the (π, π) point with increasing energy at the rate of the spin-wave velocity of the parent compounds. The spectrum is distinct from the spin-waves in two important ways: 1) the excitations are not resolution-limited; 2) there are no the outward branches. Such a spin excitation spectrum previously has been observed in itinerant spin-density-wave antiferromagnets such as elemental metal Cr⁵ and strongly correlated metal V_{2-y}O_3 ⁶, and the single-lobed dispersive continuum is referred as the Fincher-Burke mode. A self-consistent theory has been developed by Moriya and others to describe the mode⁷, and quantitative agreement has been achieved for three-dimensional itinerant antiferromagnets⁶. Itinerant theories have also been developed to account for the Fincher-Burke-like modes in superconducting cuprates⁸.

Sandwiched between the parent antiferromagnetic insulator and the high- T_C superconductor in the phase diagram of LSCO is a distinct doping regime from $x = 0.02$ to 0.05 ⁹. Cuprates in the regime are insulators without the long-range Néel order, and a spin-glass transition occurs at $T_f \lesssim 10$ K^{10,11}. This doping range is often referred to as the spin-glass regime, although the spin-glass phase extends to both lower and higher dopings in the Néel and superconducting states. Magnetic correlations were extensively investigated and regarded as being *commensurate*, as in the parent compound^{12,13}. However, with improved single-crystal samples, mag-

netic correlations show a novel *incommensurate* doublet, which also differs distinctly from the quartet in the superconductors^{9,14}. In this paper, we report that spin excitations of $\text{La}_{1.95}\text{Sr}_{0.05}\text{CuO}_4$ in the *insulating* spin-glass regime are also composed of the Fincher-Burke modes, originating from the incommensurate doublet, with a velocity the same as in superconducting LSCO. Although cuprates in the spin-glass regime are insulators, they are not the usual band insulators, and part of the Fermi surface may have survived^{15,16}. It would be interesting to investigate whether the Fincher-Burke modes reported here can be accounted for by extending theories for similar spin excitations of superconducting cuprates.

Meanwhile, for quasi-two-dimensional (2D) spin $S=1/2$ cuprates, the temperature range where spin fluctuations are investigated is within $T \ll J/k_B \sim 1000$ K¹⁷, where classical statistical mechanics has to be replaced by quantum statistical mechanics¹⁸. The general scaling argument of 2D quantum statistical systems leads to a prediction for samples which are not exactly at a quantum critical point (QCP) that for $T \ll J/k_B$ but above a low-temperature limit T_X , the energy scale for 2D spin fluctuations at long wavelengths is $k_B T$ ^{18,19}. Hence, for $T_X < T \ll J/k_B$, the spin excitation spectrum follows the ω/T scaling¹⁹, which is not a robust feature of the Moriya theory⁷. For $T < T_X$, a constant energy gap is predicted¹⁹. We test these predictions against the distinct incommensurate spin excitations from the doublet in $\text{La}_{1.95}\text{Sr}_{0.05}\text{CuO}_4$. We also compare our results with previous investigations of incommensurate spin fluctuations from the quartet in superconducting cuprate²⁰ and commensurate ones at the (π, π) point in insulating cuprate²¹. Our data support the scaling above T_X but no gap is observed below T_X . Surprisingly, scaling analysis of the \mathbf{q} and ω dependent spin excitation spectra indicates that $\text{La}_{1.95}\text{Sr}_{0.05}\text{CuO}_4$ and optimally doped LSCO are similarly distant from the QCP.

A single piece of $\text{La}_{1.95}\text{Sr}_{0.05}\text{CuO}_4$ crystal of 5.2 g was used in this work. It was grown using a traveling-solvent floating-zone method as described previously^{9,14}. We use the orthorhombic $Cmca$ unit cell ($a = 5.338\text{\AA}$, $b = 13.16\text{\AA}$, $c = 5.404\text{\AA}$ at 1.5 K) to describe the \mathbf{q} -space for measurements at NIST using the cold neutron triple-axis spectrometer SPINS. The sample temperature was controlled by a pumped He^4 cryostat. The horizontal collimations before and after the sample were both $80'$, and a Be filter cooled by liquid nitrogen was used after the sample to reduce higher order neutrons passing through the pyrolytic graphite (002) used for both monochromator and analyzer. The intensity of magnetic neutron scattering was counted against a flux monitor placed before the sample in a fixed $E_f = 5$ meV configuration and normalized to yield $S(\mathbf{q}, \omega)$ in absolute units. Such a cold neutron spectrometer readily resolves the incommensurate doublet near (100), i.e., the (π, π) point (see Fig. 1), while it is difficult to resolve the doublet using a thermal neutron triple-axis spectrometer due to its coarser resolution. Hence, we will present only the cold neutron scattering results here.

We first present the *nominal* elastic signal at various temperatures. Fig. 1(a) shows constant-energy $\hbar\omega=0$ scans through the incommensurate doublet from 1.2 to 80 K. The sharp peak at (100) is due to higher-order diffraction of (200). Its width indicates the instrument resolution. The magnetic doublets at $\mathbf{q}_{IC}=(1,0,\pm 0.058(2))$ are obviously broader than the resolution. The deconvoluted peak width yields the in-plane correlation length for the nominally elastic spin correlations, $\xi_{\square} = 34(2)\text{\AA}$ at 1.2 K, about 9 nearest-neighbor Cu spacings. With increasing temperature, the doublet monotonically decreases in intensity without appreciable change in either the peak width or position. Above ~ 20 K, the doublet disappears, consistent with previous studies⁹.

At finite energies, however, the temperature dependence of the doublet is entirely different from that at $\hbar\omega = 0$. Fig. 1(b) shows constant-energy $\hbar\omega=0.5$ meV scans measured in the same temperature range. Instead of monotonically decreasing, the intensity first increases, reaches a maximum between 15 and 20 K, and then decreases with further rising temperature. The intensity at the peak shoulder, e.g., at $\mathbf{q} = (1, 0, 0.2)$, in Fig. 1(a)-(b) measures a temperature-independent background, which has been subtracted in Fig. 1(c). Note that at 1.2 K, $S(\mathbf{q}, \omega)$ at 0.5 meV is more than one order of magnitude weaker than at $\hbar\omega = 0$. This reflects the fact that the energy spectrum of $S(\mathbf{q}, \omega)$ shows a prominent sharp “central peak” at $\omega = 0$ at low temperatures, see Fig. 1(c). The “central peak” is energy-resolution-limited at the SPINS spectrometer, with the full-width-at-half-maximum (FWHM) of 0.3 meV. However, the nominal elastic signal from $\text{La}_{1.95}\text{Sr}_{0.05}\text{CuO}_4$ is not truly static at $T > T_g \approx 5$ K as determined by our μSR measurements, which has an energy resolution of $\sim 10^{-6}$ meV. Details of the μSR study will be published elsewhere. Similar “central peak” phenomenon has been reported

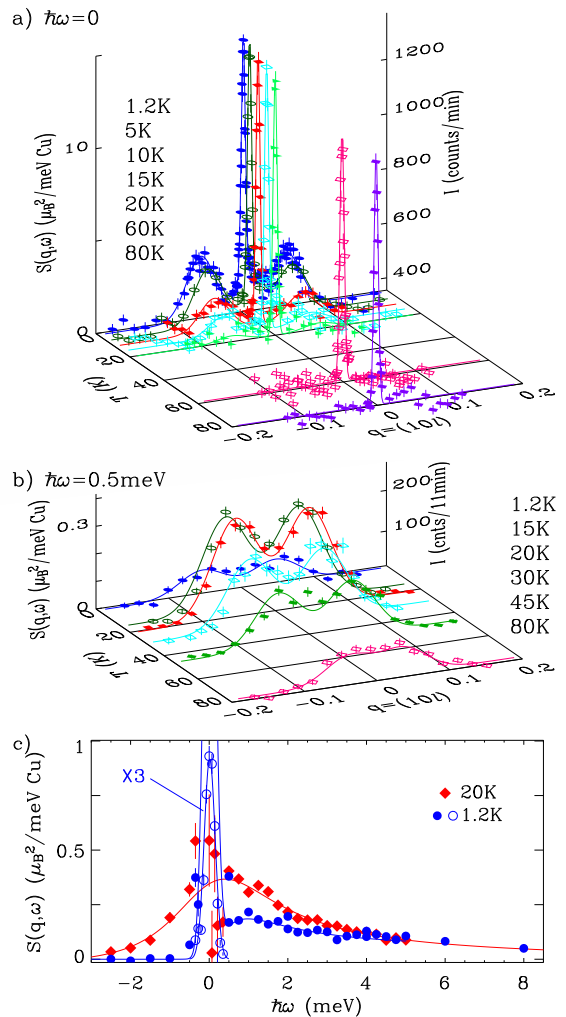


FIG. 1: (color online) The generalized spin correlation function $S(\mathbf{q}, \omega)$ as a function of \mathbf{q} along the c -axis measured at (a) $\hbar\omega = 0$ and (b) 0.5 meV, respectively, at various temperatures. (c) $S(\mathbf{q}, \omega)$ as a function of energy at $\mathbf{q} = (1, 0, 0.05)$ and at 1.2 and 20 K, respectively. The “central peak” at 1.2 K is also shown on a 1/3 scale with open circles. Background has been subtracted in (c).

for Li-doped La_2CuO_4 and $\text{YBa}_2\text{Cu}_3\text{O}_{6+x}$, and the very slow spin dynamics is attributed to a partial spin-glass transition^{22,23}.

What is the energy dependence of the doublet? Fig. 2(a) shows scans at various energies at 20 K. Below 3 meV, the two incommensurate peaks are clearly distinguishable. As energy increases, the doublet merges into a flat-top peak. The scans in Fig. 2(a) can be fitted using two gaussians of the same width. The peak positions are shown as the black circles in Fig. 2(b). The dispersion is consistent with the inner branches of spin-waves (solid lines)¹⁷. The same dispersion rate has been reported for superconducting $\text{La}_{2-x}\text{Sr}_x\text{CuO}_4$ ($x = 0.10$ and 0.16)². The shaded area in Fig. 2(b) covers the FWHM, which grows slowly with energy from $0.089(3) \text{\AA}^{-1}$ at 0.5 meV.

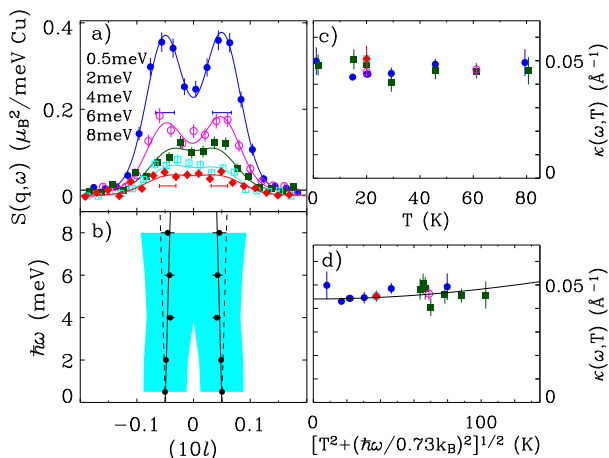


FIG. 2: (color online) (a) Constant- $\hbar\omega$ scans at 20 K. The solid lines are two equal-width Gaussians. The horizontal bars indicate instrument resolution (FWHM). (b) The double peak positions. The shaded area represents the FWHM. The spectral shape strongly resembles that for $\text{La}_{1.84}\text{Sr}_{0.16}\text{CuO}_4^2$ and $\text{V}_{1.97}\text{O}_3^6$. The lines denote the spin-wave branches with a velocity of 850 $\text{meV}\text{\AA}$ of $\text{La}_2\text{CuO}_4^{17}$. The FWHM/2 measured at those energies listed in (a) is shown as a function of temperature in (c) and reduced temperature in (d).

The width is comparable to that for the $x = 0.16$ sample. Because of the smaller doublet separation, the merge of the peaks occurs at ~ 4 meV, much lower than at ~ 40 meV for $\text{La}_{1.84}\text{Sr}_{0.16}\text{CuO}_4^2$. Thus, despite very different ground states and spatial spin correlations, insulating and superconducting LSCO share the common Fincher-Burke spectral shape.

Now we turn to examination of scaling behavior of spin excitations. Historically, it was done in the spin-glass regime through the local spin correlation function $S(\omega) = \int d\mathbf{q} S(\mathbf{q}, \omega)$ using cuprate samples showing *commensurate* spin correlations^{12,13}. It is re-examined here with the very different *incommensurate* spin correlations of our improved sample. The imaginary part of the local dynamic magnetic susceptibility relates to $S(\omega)$ by the fluctuation-dissipation theorem

$$\chi''(\omega) = \pi(1 - e^{-\hbar\omega/k_B T})S(\omega). \quad (1)$$

Fig. 3 shows $\chi''(\omega)$ from 1.2 to 80 K, which is well described by the Debye relaxor model

$$\chi''(\omega) = \frac{\chi_0(\hbar\omega/\Gamma)}{1 + (\hbar\omega/\Gamma)^2}, \quad (2)$$

where χ_0 is the local staggered static magnetic susceptibility, and Γ the spin relaxation constant. In previous studies^{12,13}, the local $\chi''(\omega)$ was modeled by

$$\chi''(\omega) = I(\omega) \arctan[a_1(\hbar\omega/k_B T) + a_2(\hbar\omega/k_B T)^2]. \quad (3)$$

The arctan function is stipulated by the marginal Fermi liquid theory^{12,24}, but $I(\omega)$ has no determined analytic form¹³. Hence, we opt for the well-known Debye relaxor

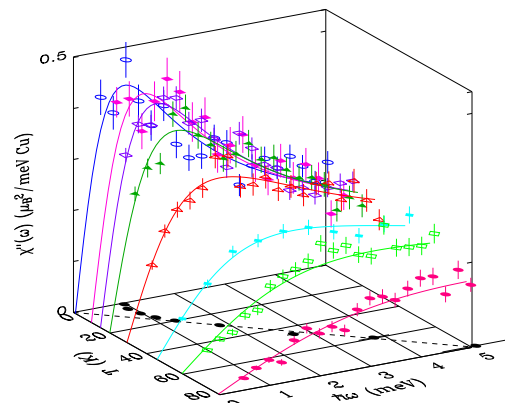


FIG. 3: (color online) The local dynamic magnetic susceptibility $\chi''(\omega)$ measured at various temperatures. The solid lines are the least-square fit to Eq. (2). The relaxation constant Γ is shown on the $\hbar\omega$ - T plane as a function of T , and departs from the dashed line $\Gamma = 0.73k_B T$ below $T_X \approx 16$ K.

model, Eq. (2), to fit our data. The Debye relaxor model has also successfully described measured $\chi''(\omega)$ of insulating $\text{La}_2\text{Cu}_{0.94}\text{Li}_{0.06}\text{O}_4$, which has *commensurate* magnetic correlations²¹.

On the base plane of Fig. 3, the spin relaxation constant Γ obtained from the least-squares fit is shown as a function of temperature. The good instrument resolution, 0.3 meV (FWHM), has a negligible effect during fitting. One interesting result is that $\Gamma = 0.73(2)k_B T$ for temperatures above $T_X \approx 16$ K. Hence, when $\chi''(\omega)$, normalized by its maximum $\chi_0/2$ at $\hbar\omega = \Gamma$, is plotted as a function of $\hbar\omega/k_B T$, Eq. (2) dictates that all data collected above T_X collapse onto a single universal curve $y = 2/[1 + (x/0.73)^2]$ and Fig. 4(a) bears this out. The result is commonly referred to as the ω/T scaling, and $\Gamma/k_B T = O(1)$ is a hallmark of quantum magnetic theory^{18,19}. For $T < T_X$, Fig. 3 shows that Γ departs from the proportionality to temperature. Consequently, the low temperature data would not follow the scaling curve, as demonstrated by Fig. 4(b). Note that the spectral function Eq. (2) does not become gapped below T_X , contrary to non-random quantum theory¹⁹, but can be explained by dopant scattering^{25,26}.

The ω/T scaling and its departure below T_X shown in Fig. 4 for $\text{La}_{1.95}\text{Sr}_{0.05}\text{CuO}_4$ bears a striking similarity to what reported for $\text{La}_2\text{Cu}_{0.94}\text{Li}_{0.06}\text{O}_4^{21}$. The two cuprates have similar hole concentration and develop spin-glass at similar T_g . However, they differ in several important ways: i) The dopants are out of the CuO_2 plane in the Sr compound, but directly replace Cu^{2+} in the Li compound. ii) The former becomes a superconductor with additional 0.5% more holes, but the latter always remains an insulator. iii) Magnetic correlations are incommensurate in the former, but commensurate in the latter. iv) The in-plane correlation length $\xi_{\square} \simeq 34(2)\text{\AA}$ for the glassy spin component in the former, but $\xi_{\square} \gg 274\text{\AA}$ in the latter, and the $\kappa(\omega, T)$ shown in Fig. 2(c) is more than double that in the latter²². v)

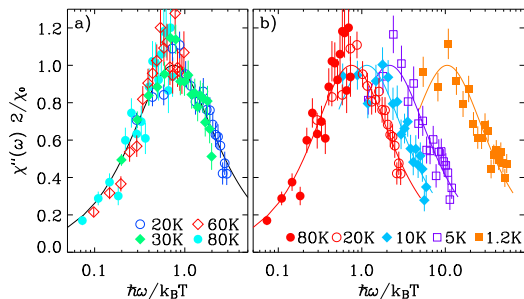


FIG. 4: (color online) The normalized local dynamic magnetic susceptibility $\chi''(\omega)2/\chi_0$ as a function of $\hbar\omega/k_B T$. (a) The ω/T scaling is followed for data taken above $T_X \simeq 16$ K. The solid curve is the scaling function $y = 2/[1 + (x/0.73)^2]$. (b) Data taken below T_X does not follow the scaling function.

$\Gamma/k_B T = 0.73$ for the former, and 0.18 for the latter²¹. In spite of these differences, Γ saturates at $\Gamma_0 \sim 1$ meV and $\chi''(\omega)$ becomes essentially T -independent (see Fig. 3) for both cuprates below T_X . As a consequence, Eq. (1) requires a reduced $S(\omega)$ at low energies when the temperature decreases below T_X , as observed in Fig. 1(b) and (c), in sharp contrast to a magnet at the QCP.

Scaling of spin excitations has also been examined near the optimal doping for $\text{La}_{1.86}\text{Sr}_{0.14}\text{CuO}_4$ ²⁰. The material is concluded to be near a QCP, namely, $T_X \rightarrow 0$, with some caveat²⁷. The χ''_P/ω in [20], equaling to χ_0/Γ of Eq. (2), would saturate below T_X , but $T_C = 35$ K sets the upper limit for measurable T_X in $\text{La}_{1.86}\text{Sr}_{0.14}\text{CuO}_4$. Hence it cannot be determined whether $\text{La}_{1.86}\text{Sr}_{0.14}\text{CuO}_4$ or $\text{La}_{1.95}\text{Sr}_{0.05}\text{CuO}_4$ is closer to a QCP with a lower T_X .

Another method to assess the distance from the QCP is to examine the width of constant- $\hbar\omega$ scans, see Fig. 2(c). Adapting the ansatz in [20], the $\kappa(\omega, T)$ plotted as a function of a reduced temperature better collapses our data in Fig. 2(d), and the solid line is

$$\kappa(\omega, T)^2 = \kappa_0^2 + (k_B T/c)^2 [1 + (\hbar\omega/0.73k_B T)^2], \quad (4)$$

where $\kappa_0 = 0.044(1)\text{\AA}^{-1}$ and $c = 4(1) \times 10^2$ meV \AA . At the QCP, κ_0 is expected to be zero, and its value for $\text{La}_{1.95}\text{Sr}_{0.05}\text{CuO}_4$ is comparable to κ_0 in the superconducting state, but narrower than κ_0 at 40 K in the normal state for $\text{La}_{1.84}\text{Sr}_{0.16}\text{CuO}_4$ ². Hence, $\text{La}_{1.95}\text{Sr}_{0.05}\text{CuO}_4$ and the optimally doped LSCO with a short $1/\kappa_0$, about 6 Cu-Cu spacings, seem equally distant from the QCP.

In conclusion, the Fincher-Burke modes, the broad and dispersive spin excitations of itinerant antiferromagnets, are observed in the spin-glass regime of $\text{La}_{2-x}\text{Sr}_x\text{CuO}_4$. Theoretical understanding of similar excitation modes in superconducting cuprates now has an added task in the insulators. Befitting to the generality of its theoretical argument, the ω/T scaling is shown to be valid for a new type of cuprates above T_X . Spin excitations below T_X remain gapless contrary to the prediction of non-random quantum theory. The spin-glass transition at finite doping introduces an extra component of slow spin fluctuations. It would be interesting to explore whether the glassy state^{22,23,28}, limiting the correlation length of the rest of spins, is responsible for the equal distance from the QCP for $\text{La}_{1.95}\text{Sr}_{0.05}\text{CuO}_4$ and $\text{La}_{1.84}\text{Sr}_{0.16}\text{CuO}_4$.

Work at LANL is supported by U.S. DOE, and SPINS partially by NSF under Agreement No. DMR-0454672.

¹ J. M. Tranquada, in *Handbook of High-Temperature Superconductivity*, edited by J. R. Schrieffer (Springer, Berlin, 2007), p. 257.
² N. B. Christensen, D. F. McMorrow, H. M. Rønnow, B. Lake, S. M. Hayden, G. Aeppli, T. G. Perring, M. Mangkorntong, M. Nohara, and H. Takagi, *Phys. Rev. Lett.* **93**, 147002 (2004).
³ S. M. Hayden, H. A. Mook, P. Dai, T. G. Perring, and F. Doğan, *Nature (London)* **429**, 531 (2004).
⁴ J. M. Tranquada, H. Woo, T. G. Perring, H. Goka, G. D. Gu, G. Xu, M. Fujita, and K. Yamada, *Nature (London)* **429**, 534 (2004).
⁵ C. R. Fincher, G. Shirani, and S. A. Werner, *Phys. Rev. B* **24**, 1312 (1981).
⁶ W. Bao, C. Broholm, S. A. Carter, T. F. Rosenbaum, G. Aeppli, S. F. Trevino, P. Metcalf, J. M. Honig, and J. Spalek, *Phys. Rev. Lett.* **71**, 766 (1993); W. Bao, C. Broholm, J. M. Honig, P. Metcalf, and S. F. Trevino, *Phys. Rev. B* **54**, R3726 (1996).
⁷ T. Moriya, *Spin Fluctuations in Itinerant Electron Magnetism* (Springer-Verlag and Berlin, 1985).
⁸ A. Abanov and A. V. Chubukov, *Phys. Rev. Lett.* **83**, 1652 (1999); U. Chatterjee et al., *Phys. Rev. B* **75**, 172504 (2007).

⁹ M. Fujita, K. Yamada, H. Hiraka, P. M. Gehring, S. H. Lee, S. Wakimoto, and G. Shirane, *Phys. Rev. B* **65**, 64505 (2002).
¹⁰ B. J. Sternlieb, G. M. Luke, Y. J. Uemura, T. M. Rise-man, J. H. Brewer, P. M. Gehring, K. Yamada, Y. Hidaka, T. Murakami, T. R. Thurston, et al., *Phys. Rev. B* **41**, 8866 (1990).
¹¹ F. C. Chou, F. Borsa, J. H. Cho, D. C. Johnston, A. Lascialfari, D. R. Torgeson, and J. Ziolo, *Phys. Rev. Lett.* **71**, 2323 (1993).
¹² B. Keimer, N. Belk, R. J. Birgeneau, A. Cassanho, C. Y. Chen, M. Greven, M. A. Kastner, A. Aharony, Y. Endoh, R. W. Erwin, et al., *Phys. Rev. B* **46**, 14034 (1992).
¹³ M. Matsuda, R. J. Birgeneau, Y. Endoh, Y. Hidaka, M. A. Kastner, K. Nakajima, G. Shirane, T. R. Thurston, and K. Yamada, *J. Phys. Soc. Jpn* **62**, 1702 (1993).
¹⁴ S. Wakimoto, G. Shirane, Y. Endoh, K. Hirota, S. Ueki, K. Yamada, R. J. Birgeneau, M. A. Kastner, Y. S. Lee, P. M. Gehring, et al., *Phys. Rev. B* **60**, R769 (1999).
¹⁵ M. L. Tacon, A. Sacuto, A. Georges, G. Kotliar, Y. Gallais, D. Colson, and A. Forget, *Nature Physics* **2**, 537 (2006).
¹⁶ T. Yoshida, X. J. Zhou, T. Sasagawa, W. L. Yang, P. V. Bogdanov, A. Lanzara, Z. Hussain, T. Mizokawa, A. Fujimori, H. Eisaki, et al., *Phys. Rev. Lett.* **91**, 027001 (2003).

- ¹⁷ S. M. Hayden, G. Aeppli, R. Osborn, A. D. Taylor, T. G. Perring, S.-W. Cheong, and Z. Fisk, *Phys. Rev. Lett.* **67**, 3622 (1991).
- ¹⁸ D. Belitz, T. R. Kirkpatrick, and T. Vojta, *Rev. Mod. Phys.* **77**, 579 (2005).
- ¹⁹ S. Sachdev and J. Ye, *Phys. Rev. Lett.* **70**, 3339 (1993).
- ²⁰ G. Aeppli, T. E. Mason, S. M. Hayden, H. A. Mook, and J. Kulda, *Science* **278**, 1432 (1997).
- ²¹ W. Bao, Y. Chen, Y. Qiu, and J. L. Sarrao, *Phys. Rev. Lett.* **91**, 127005 (2003).
- ²² Y. Chen, W. Bao, Y. Qiu, J. E. Lorenzo, J. L. Sarrao, D. L. Ho, and M. Y. Lin, *Phys. Rev. B* **72**, 184401 (2005).
- ²³ C. Stock, W. J. L. Buyers, Z. Yamani, C. L. Broholm, J.-H. Chung, Z. Tun, R. Liang, D. Bonn, W. N. Hardy, and R. J. Birgeneau, *Phys. Rev. B* **73**, 100504(R) (2006).
- ²⁴ C. M. Varma, P. B. Littlewood, S. Schmitt-Rink, E. Abrahams, and A. E. Ruckenstein, *Phys. Rev. Lett.* **63**, 1996 (1989).
- ²⁵ S. Sachdev, A. V. Chubukov, and A. Sokol, *Phys. Rev. B* **51**, 14874 (1995).
- ²⁶ Y. L. Liu and Z. B. Su, *Phys. Lett. A* **200**, 393 (1995).
- ²⁷ S. Chakravarty, *Science* **278**, 1412 (1997).
- ²⁸ C. Panagopoulos, A. P. Petrovic, Hillier, J. L. Tallon, C. A. Scott, and A. P. Rainford, *Phys. Rev. B* **69**, 144510 (2004).